

Supplementary Information

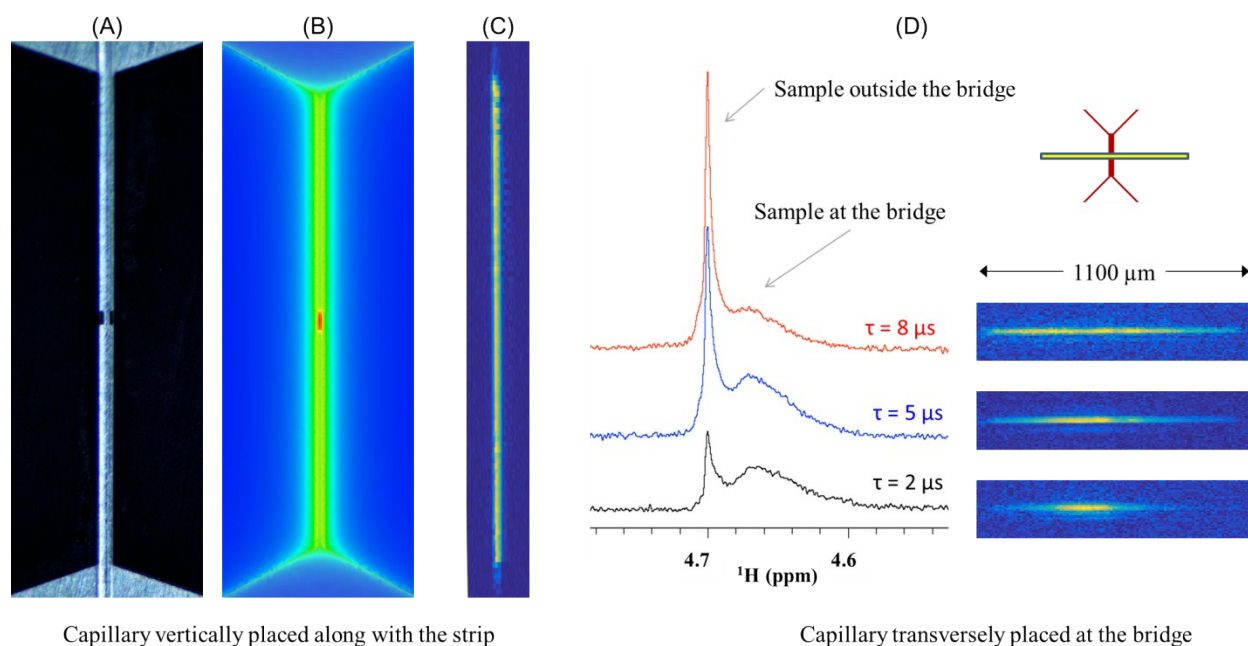


Figure S1. Effective volume of a microslot-style detector. (A) A capillary filled with DI H_2O placed vertically on top of the detector with a bridge at the center (refer to our previous work¹ for details of detector design and fabrication). Note that the bridge is 200 μm long while the entire strip is 7 mm long. (B) FEM simulation shows that RF field strength reaches its maximum at the bridge, dramatically decreases to half of the maximum on the strip, and further drops to nearly zero outside of the strip. (C) Spin-echo MRI sagittal image of the capillary filled with DI H_2O . Surprisingly, the image does not demonstrate a greater intensity at the center. This may be due to the following: 1) the 90° pulse width is optimized for all detectable signals, while the signal from the 6.8 mm long strip dominates over the signal from the 0.2 mm long bridge; 2) B_0 inhomogeneity introduced by the susceptibility mismatch between the bridge and the strip further reduces the signal intensity at the bridge. (D) A capillary with a water plug of 1.1 mm

encapsulated between two FC-43 plugs was positioned transversely at the bridge, and a shimmed ^1H spectrum (left side of the panel) was collected at varying pulse durations with corresponding spin-echo MRI axial image (right side of the panel). The deviation of MRI image from FEM simulation is clear. The sample at the bridge produces a broader signal than the sample outside of the bridge due to the stronger susceptibility mismatch at the bridge area. When the pulse width increases from $2\ \mu\text{s}$ to $8\ \mu\text{s}$ at a power of $1\ \text{W}$, the signal from outside the bridge rises dramatically due to the weaker RF field at this area, and MRI image shows an increase in the effective sample length from $500\ \mu\text{m}$ to $1100\ \mu\text{m}$ with the high intensity region from $250\ \mu\text{m}$ to $800\ \mu\text{m}$, indicating that the sample can be detected from the areas where the RF field strength is estimated close to zero in the FEM simulation.

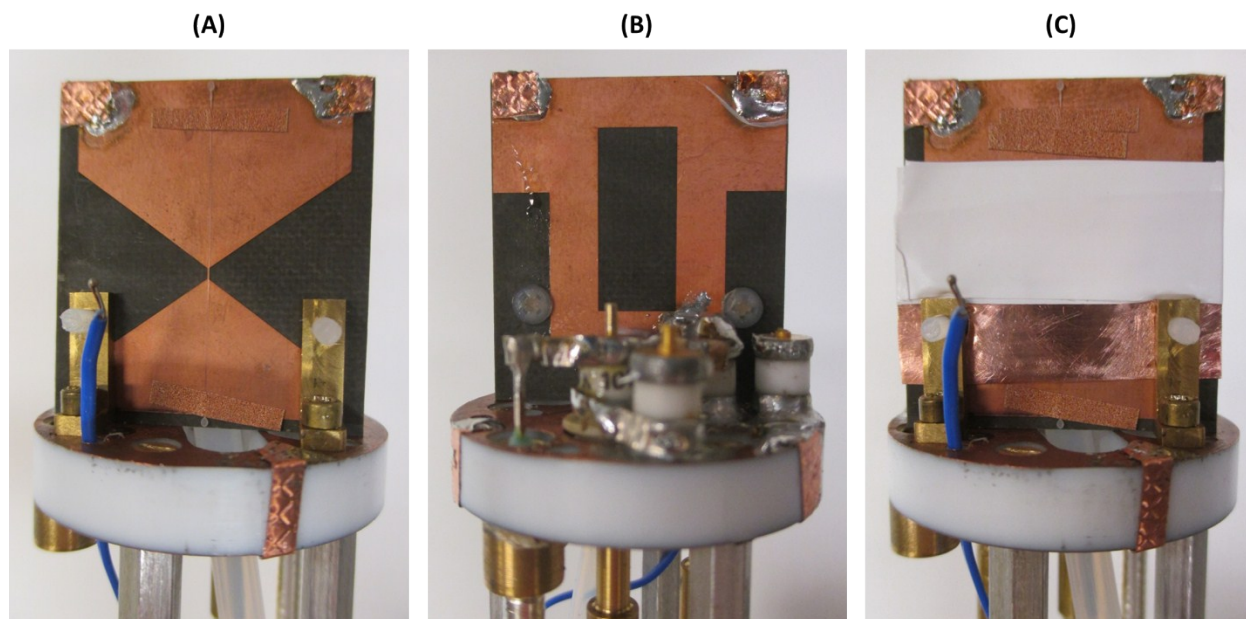


Figure S2. Narrow-bore probehead with a detector of length $1\ \text{mm}$ and width $150\ \mu\text{m}$. (A) Flat-wire detector fabricated on Rogers 5880 substrate, with the sample-carrying capillary (ID $50\ \mu\text{m}$

/ OD 80 μm) positioned directly on top of the strip. The blue wire is a thermocouple and the white tubing is a gas inlet for temperature regulation. (B) Copper on the back side of the board, with capacitors soldered at the lower right corner. (C) Microstrip detector with the sample located between the strip conductor and the ground plane. The board is covered with a layer of Teflon tape as insulator and another layer of rolled copper foil as ground plane. The central white band is Teflon tape used to press down the copper ground plane.

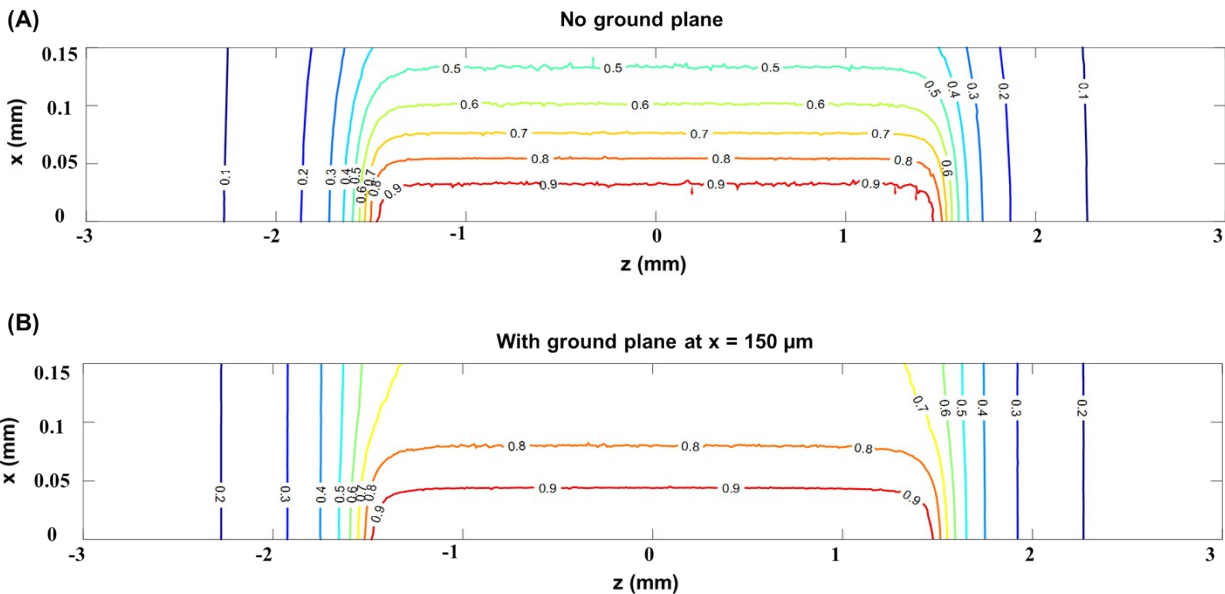


Figure S3. Contour plots of RF field maps on the yz plane at the center of the strip ($x = 0$) for a microstrip detector with a length of 3 mm at an RF frequency of 500 MHz, with no ground plane (A) and with a ground plane at $x = 150 \mu\text{m}$ (B). It is clear that the RF field is much stronger and more homogeneous with a ground plane at a distance of 150 μm . Note that x and z axes of the plots are out of scale in order to provide a better view of the contours.

Table 1. RF performance of the detectors with varying strip length and sample length. The simulation results of $A_{810^\circ}/A_{90^\circ}$ are listed in the parentheses for a back-to-back comparison.

Strip length; Sample length	$A_{810^\circ}/A_{90^\circ}$		90° pulse duration at 0.25 W (μs)		RF conversion efficiency ($\text{mT}/\sqrt{\text{W}}$)	
	No ground	With ground	No ground	With ground	No ground	With ground
7 mm; full	0.70 (0.67)	0.78 (0.77)	5.62	4.75	2.09	2.47
1 mm; full	0.50 (0.51)	0.50 (0.60)	4.65	3.12	2.52	3.76
1 mm; 0.5 mm	0.50 (0.63)	0.75 (0.85)	4.65	2.81	2.52	4.18

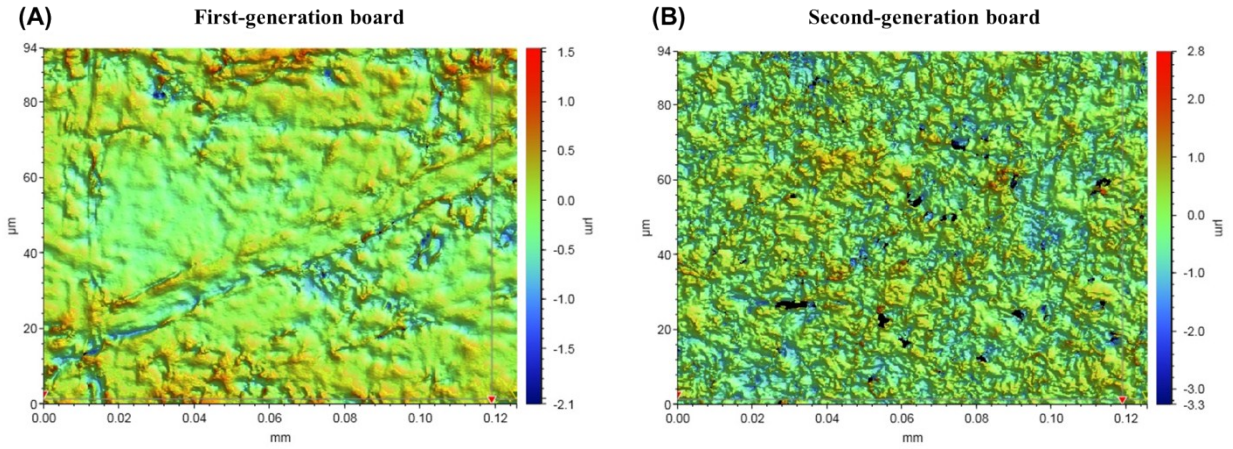


Figure S4. 3D surface profiles of the microstrips on the first- (A) and second-generation (B) boards. The surface RMS roughness was measured to be $0.19 \mu\text{m}$ and $0.35 \mu\text{m}$, respectively.

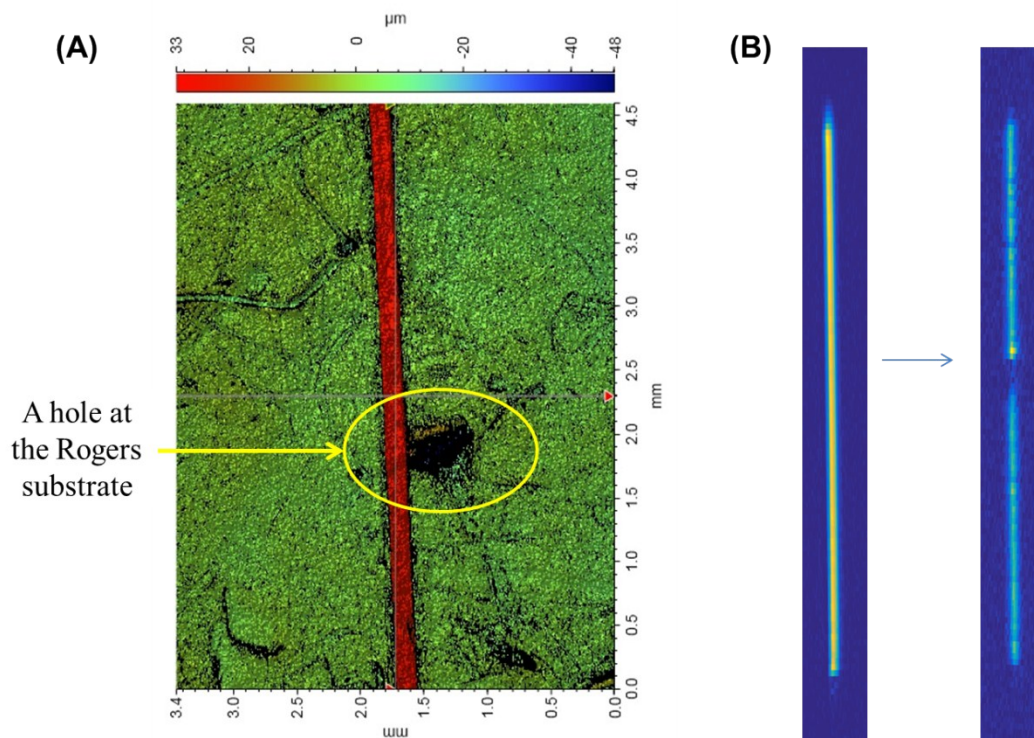


Figure S5. (A) 3D surface profiles of a first-generation microstrip, highlighting the hole with a diameter of around 0.5 mm and a depth of 50 μm accidentally made in the Rogers substrate close to the center of the strip. (B) Sagittal 2D spin-echo MRI image (yellow corresponds to high intensity and blue corresponds to low intensity) of a capillary (quartz, ID 80 μm / OD 100 μm) filled with DI H_2O , before and after the hole was made, indicating the significant B_0 inhomogeneity induced by the hole on the substrate.